Technical Report

MIT Sea Grant College Program

Massachusetts Institute
of Technology
Cambridge, Massachusetts
02139

MODELLING OF SYNTHETIC FIBER ROPES DETERIORATION CAUSED BY INTERNAL ABRASION AND TENSILE FATIGUE

By Moon Hwo Seo, Stanley Backer and
John F. Mandell

MITSG 90-18

Sea Grant College Program
Massachusetts Institute of Technology
Cambridge, Massachusetts 02139

Grant No: NA86AA-D-SG089
Project No: RT-11

ABSTRACT

In this study models have been formulated for prediction of service life of synthetic fiber double braided rope based on geometrically ideal rope structures. Two experimentally determined rope deterioration factors have been considered: tensile creep induced fatigue and wear /abrasion behavior of constituent fibers. Model based predictions agree reasonably well with tensile fatigue tests conducted at high loading levels as well as in an extended low load test series. At the high loads, tensile creep dominates, while at the low cycling tensions internal wear determines rope life. The model is designed to treat both deployment conditions and gives insight to the interaction of tensile fatigue, wear, and the structural mechanics of rope.

CONTENTS

1. INTRODUCTION

Interest in failure mechanisms in synthetic fiber rope has increased in proportion to the number of serious accidents which have occurred during marine usuage. For the relatively high strain energy stored in synthetic fiber rope prior to failure frequently leads to intense snapback and whipping action capable of causing considerable damage to equipment and critical injury to personnel.

There has been considerable active research related to actual loading conditions in the marine environment[1, 2], to tensile fatigue life[3, 4, 5, 6, 7], and to theoretical modelling of structural mechanics and experimental verifications[12, 13, 17, 18, 19, 20]. These data relate to rope failure at any structural point such as mid span failure and eye splice zone failure. Since the low load tensile fatigue tests involve longer than acceptable time span, most tests have been done at tensile loads higher than 35 % of nominal breaking strengths. The results show a wide band of life cycles for both nylon and PET ropes. PET rope showed longer life than nylon rope in these testing range.

In practice, however marine ropes are employed with safety factors of 5 to 10 as recommended by rope manufactures, and thus their normal working loads range from 10 to 20 % of rated dry breaking strengths. In selected cases the cyclic load levels in practice are far less. For example the measured tensions of a shallow water mooring line show that the average loading level can less than 3 % of its nominal breaking strength and the magnitude of additional load fluctuation is less than 10 % of its breaking strength levels during most of its deployment period(6 months)[1]. Therefore, the conventional tensile fatigue conditions reported above are a great deal more severe than real life loading conditions and there is no justification for the linear extension of these severe test results to the low axial load cycling cases such as actual mooring or towing conditions.

Extensive pathological studies have been conducted on cyclic tensile fatigue tested lines as well as marine deployed lines[9]. Such studies on mooring lines deployed in the shallow water[1] and at considerable depths manifests significant internal fiber wear failures[9]. In buoy mooring lines which were not subjected to external abrasion nor to photochemical degradation, it was found that residual strength decreased essentially linearly with deployment time. Observation under the Scanning Electron Microscope(SEM) revealed extensive internal fiber abrasion resulting in reduction in fiber, yarn, and rope strengths.

Similar SEM studies of double braided PET ropes tensile cycled to 35% of breaking strength showed considerable internal wear damage[8]. Likewise nylon 6, nylon 66, and PET plaited ropes cycle tested at 50 and 70 % of breaking strength manifested severe internal wear and fiber abrasion. The latter were judged to have failed by tensile creep.

Recently Mandell[21] proposed a rope life model and estimated exponents which provided best curve fits to the experimental results. However, there is no physical explanation for these changing exponents, thus making it more difficult to predict the total rope S-N curve shape from this first model. In the current study, a second model of synthetic fiber rope deterioration life prediction has been proposed for double braided structures treating both internal and external wear combined with fiber tensile fatigue failure.

2. ROPE DETERIORATION MODEL

For the structural modelling of a strand in double braided rope, the location of a position along the strand can be represented as a spacial curve consisting of a sinusoidal undulation superposed on a circular helix[12] as depicted in Fig. 1.

T he local strand strain is estimated from the geometrical relationships between the length of the strand axis and the rope length between two parallel rope

cross sections considered both before and after rope tension loading. Two friction constraints among the strands in a rope cross section are treated; infinite friction and zero friction. For the infinite friction case, local strand strain can be estimated via differential geometry and total strand strain then becomes the summation of local strand segment extensions per unit helix cycle. For the zero friction case, local strand strain is the same along the strand. The corresponding strand stress can then be estimated from constitutive property of each strand. Total rope load can be estimated by the summation of axial components of each strand tension in a rope cross section. An extensive comparison of predicted values and experimental results has been conducted on specially made 7/8 inch diameter nylon 66 and PET ropes[12]. Results showed that predicted stress-strain curves of nylon 66 rope shows better agreement to measured values than those of PET ropes. At the same time, lateral pressure and relative movement between the strands were estimated.

When the rope is viewed as a gradually deteriorating structure, it can be modelled as a collection of segments of fiber bundles which receive axial tension as well as lateral pressure due to the local strand curvature. Each small segment of a strand in a loaded rope can be simplified as a differential deterioration model as shown in Fig. 2. When there is cyclic axial tension present in the strand, all its fibers will be subjected to an axial tensile cyclic load which will induce tensile fatigue in all fibers. However, at contact zone of two strands, there will be relative movement between two opposing strands with high pressure due to the strand curvatures. Thus, the cyclic tension along the strand axis induces surface fiber wear as well as tensile fatigue of fibers in the strand body.

Since the rope is primarily a tensile structure, the major application is in applying axial tension with free transverse movement, as in towing and mooring. This mode of loading allows the rope to vibrate laterally at its resonant frequencies even though there is no apparent external source of vibration outside of fluid induced

strumming. Since such vibration of a slender body induces local bending, relative movement between the rope components may occur at the same time[12].

In addition to the assumption associated with structural modelling[12], the following assumptions are added to predict the rope deteriorations.

(a) Each layer of the rope consists of identical strands which have a rectangular cross section of uniform fiber bundles.

(b) Internal wear is assumed to occur uniformly along the yarn surface on the highest curvature side.

(c) Filaments are assumed to be worn off layer by layer and the width of the contact zone either remains constant or else is varied by rearranging the cross sectional position of filaments so that the ratio of bundle thickness to width is maintained constant.

(d) Tensile fatigue is assumed to proceed uniformly in the whole bundle, bwithout actual interacting with the wear process except for the cross-sectional area reduction where the wear occurs.

(e) The strand will fail either when the population of filaments break by tensile fatigue or when the entire strand is worn away.

The flow chart of the computation is shown in Fig. 3.

3. TENSILE FATIGUE AND WEAR BEHAVIOR OF NYLON AND PET FIBERS

In a separate study on the tensile fatigue behavior of textile yarns and fibers, the tensile cyclic fatigue failure life of synthetic rope fibers(Nylon 6.6. and PET) show a total creep time dependence[10, 11,]. The measured tensile fatigue life of nylon 6.6 and PET fibers and yarns in logarithmic scale shows linear relationship to the applied tensile stress above 40 - 50 % of ultimate breaking stress for nylon

6.6 fibers and above 60 % for PET fibers[10, 11].

$$\frac{\sigma_t}{\sigma_{tb}} = 1 - \frac{1}{S_t} \log t_t \tag{1}$$

where

t_t : tensile fatigue life(cumulative time to failure)

$1/S_t$: S-N slope of tensile fatigue curve

σ_{tb} : tensile breaking stress of a new filament

σ_t : maximum applied tensile stress

One of the important outcomes of this result is that tensile fatigue life of these fibers depends on the total creep time which is independent of frequency of cycling. These results suggest the applicability of a time based Miner's rule for cumulative creep damage.

From friction and wear tests of monofilaments and rope yarns[12], it was concluded that wear life of yarn is dominated by the total number of friction cycles. Yarn wear S-N curves were obtained from yarn on yarn (YOY) tests as a function of applied normal pressure.

The general pattern of measured yarn wear S-N curves can be expressed as seen in Fig. 4. This can be divided into three parts: non-linear parts at low and high axial loads and an almost linear part for moderate loads. We have developed extensive wear data for various yarns at moderate and high axial loads, but few data at very low axial loads. When the low axial load data are unavailable, we use a hyperbolic approximation to satisfy the two boundary conditions: at zero load, yarn wear failure cycles are infinite, and the tangent of the low and intermediate curves is the same where they join.

Since the high axial load data showed large deviations, the S-N curves at high axial loads are also approximated with an exponential curve based upon measured results.

(1) Low Axial Load Case

$$\log N_w = -\frac{S_{wu}\, P_1^2}{P} - C_o \tag{2a}$$

(2) Moderate Axial Load Case

$$\log N_w = -S_{wu}\, P - C_o \tag{2b}$$

(3) High Axial Load Case

$$\begin{aligned} log N_w = &- \frac{S_{wu}\, P_3 - C_o}{(1 - \mathrm{e})}(1 - \mathrm{e}^{(P-P_2)/(P_3-P_2)}) \\ &- S_{wu}\, P - C_o \end{aligned} \tag{2c}$$

where

N_w : Wear cycles to failure

S_{wu} : Slope of intermediate segment of wear S-N curve

P_1 : Normal pressure at the boundary between the low and moderate load curves

P_2 : Normal pressure at the boundary between the moderate and high load curves

P_3 : Single cycle failure normal pressure(C_{a2},Fig4)

P : Normal pressure

4. PREDICTION OF DETERIORATION S-N CURVES OF THE ROPE

In rope structures, any rope deformation can produce relative movement between the strands. The absolute magnitude of relative movements between the rope components is dependent upon the cycling load amplitude: however, the necessary and sufficient conditions for relative movement for internal wear generation are

uncertain. Pathological studies of low amplitude deployment loading[1,9] of rope suggest that internal wear can occur even at axial load amplitudes of 1-5 % of the UTS in marine environments, which may reflect the local bending effects due to sea wave action. Therefore, we assume as follows.

(a) The relative movement between the rope components occurs in every loading cycle.

(b) The cross-section of each strand consisted of square array of filaments.

(c) All the filaments in a strand have identical properties.

(d) Internal wear occurs only at the strand surfaces possessing the highest curvature.

(e) Worn off layers do not change the local strand structural curvatures.

(f) The residual strength of rope is dependent only on the weakest strand point where internal wear occurs most severely

There are many occasions when rope is subjected to external wear, i.e. relative movement between lines and other hardware such as pulleys, capstans, bollards, deck surfaces or cap rails during deploying and retrieving of mooring or towing lines, eye-splice wear during cyclic loading tests[4], and wear at capstan jaws during static tensile tests. Since by definition, external wear occurs at the rope surface, internal and external wear damage are independent of each other and can be superposed to determine total deterioration of ropes.

Obviously external wear occurs on that side of a rope which is in contact with other objects. However, since most rope strands follow helical paths, the occurrence of local damage of a strand at a particular rope section will (for the case of low friction between strands) reduce the tension bearing capacity of that same strand at nearby locations in the rope. Damage incurred on the other strands elsewhere in the low friction rope will likewise reduce their tension bearing capacity with resultant weakening of the rope. If on the other hand friction between strands

is high, damage at a given location will affect load bearing capacity of that strand for only a short distance from the damage. And if a second strand is damaged at a larger distance from the first strand damage the two damaged regimes will have minimum interaction. This localization of wear damage involves load sharing which is dependent on friction or shear stress transfer, a subject well researched in the field of composites.

When the wear zone becomes longer (though still with narrow width), the number of wear damaged strands increases and when this zone exceeds the length of single primary strand helix, the local external wear can reduce strength of all of the exposed surface strands. If the lateral pressure within the rope is not high enough to limit strand frictional slippage, this kind of external wear can be treated as a uniform external wear process. Hence, the effect of external wear on rope strength reduction can be changed by the wear zone length on the rope surface. We have considered two extreme cases: external wear at highly localized position on the rope surface, which we term local external wear and external wear with a zone which exceeds the length of the single primary strand helix which is modelled as a uniform external wear process for low friction rope models.

Comparison of Predicted Results with Experimental Rope S-N Results

In most experimental programs relating to tensile fatigue of ropes, the majority of rope failure data reported represent failures of rope terminations. Especially at low axial load cycles, most rope fails at the eye-splice as shown in Fig. 5 with severe external wear[6, 8]. In addition to this, the energy released from hysteresis generates high internal rope temperatures if the test is not run wet. Therefore, the most pertinent data to the current study comes from end of splice or mid-span failures under wet conditions. Some limited end of splice and mid-span failure data have been identified for wet nylon and wet PET ropes[6] .

First, we have compared rope mid-span failure data to the results predicted

from the rope model. From the mid-span prediction and external rope wear models, i.e. simple bundle wear cum tensile fatigue model and rope external wear model, the rope termination effects are then discussed qualitatively.

Calculations of deterioration have been conducted employing the material properties taken from measured data listed in Table 1. Both the initial strength of the rope and its deterioration rate are predicted in the model.

Table 1. The Tensile Fatigue Slopes and Wear S-N Charateristics

	Wet Nylon	Wet PET
TensileFatigue		
S-N Slope	10.0	17.4
WearProperty		
C_o	3.6	4.5
C_a, psi	18375	16850
P_1, psi	2250	200
P_2, psi	6750	9900

It is worth noting that most references do not indicate rope structure in detail, but we assumed that these ropes are three dimensionally similar to the rope set in our tests.

A) Prediction and Comparison of Mid-Span Failure

The model is used to predict both the initial strength and the S-N curve based on both creep rupture and wear data from yarn tests. Since the cycling

frequencies of the experimental data vary significantly, the comparisons should be done between the predicted and measured results with the same frequency. Fig. 6 shows two predicted S-N curves of a wet nylon rope(with Dupont 707 nylon yarn) with two testing cycling periods, 5 and 120 s/cycle, and mid-span or end of splice failure data[1, 5, 12]. Most of the experimental data fall very close to the predicted curve for creep failure. All such nylon data tends to be creep-rupture dominated, and significant effects of internal abrasion are not present. However, we predict that such ropes would become wear dominated at slightly lower cycling loads.

For the PET ropes we find mid-span failure data in only five cases, due to the dominance of external wear failures. Fig. 7 shows the predicted curve of a wet PET rope(Dupont 608 yarns) with 65 s/cycle period, compared with experimental results[4]. This result shows excellent agreement in the internal wear dominated low load zone, as well as in the creep dominated high load zone. The higher creep rupture resistance of PET(as compared with nylon) results in a shift to wear dominated behavior at higher load levels, as predicted by the model(Fig. 8). PET gives better performance than nylon under wet conditions in both the creep-rupture and wear dominated regimes, as predicted but there is an uncertain region at very low axial load.

B) Comparision of Residual Strength Predicted with Available Data

If the rope strength reduction is dominated by internal wear, the residual strength is predicted to show a gradual reduction[9]. We have predicted residual strengths based purely upon our rope model employing measured material properties. Fig. 9 gives the predicted residual strength and deterioration S-N curves of a 6 in. circumference Samson PET rope. The residual strength curve shows significant strength reduction with cycles of tensile loading (Fig. 10). The comparison of predicted and measured residual strengths is summarized in Table 2, and includes the data for a single 9-month Samson test in Fig. 9, as well as the points for core

and sheath strands and rope in Fig. 10.

Table 2. Comparison of Measured and Predicted Residual Strengths : Rope / Components

Rope S2(cycled at 25.7% UTS)

Residual Strength(%)	Rope	Core Strand	Sheath Strand
Measured	64.0	35.0	37.0
Predicted	40.5	43.6	30.0

Rope S1(cycled at 60.0% UTS)

	Rope	Core Strand	Sheath Strand
Measured[1]	0.0	84.3	77.5
Predicted	98.0	98.6	97.0

Measured Filament Residual Strength(% UTS)

	Core Filament	Sheath Filament
Rope S1	95.5	111.1
Rope S2	77.4	51.2

[1]: Strand specimens are taken from tensile fatigue failed rope.

First we compared the Samson rope cycled to 10^6 times since the final failure moments include many uncertain factors. There is about 10 % difference in residual strand strengths between predicted and measured values. However, the difference is 24 % for the rope residual strength. The measured relative residual rope strength is much higher than that of strands. This indicates either that the measured rope strength reveals fiber friction effect or non-uniform wear along the strand of actual rope since the measured strand strength reveals the strength of the weakest point of

several undulation cycles. Therefore, the comparison of residual strength of strands is more appropriate to show the difference of measured and predicted results.

If the model can predict the strand residual strength accurately, the predicted residual strength of strands should show higher values than measured values. since measured residual strength of a strand represents the strength of the weakest point and the wearing filament layer may not include the same filaments. The predicted value for the core strand shows similar trend as expected; however, the sheath shows the opposite trend. However, there is less than 10 % difference between actual data and prediction of the residual strength of strands based upon measured yarn properties and rope modelling can be accepted as providing reasonable results. The overall rope result is also well predicted if viewed on a typical semilog plot as in Fig. 9. Thus the model gives a good idea of rope lifetime and rate of strength loss in this instance, for a rope cycled for nine months and then tested for residual strength.

Rope S1 was subjected to 5000 cycles and failed during cycling. In this case, there is no indication of filament strength reduction (which does not correlate with the strand data); however, rope S2 shows correlation of fiber data and strand data. The fiber breakage position diagrams of rope S1 show no clustering, but rope S2 showed significant indications of local damage[12]. This result indicates that even though the strands of rope S2 show some strength reduction, this does not indicate gradual wear occurring during cycling. Instead, the rope likely failed from a tensile fatigue process dominated mode as the model suggests. Creep dominated failures are sudden-death in nature as noted earlier, and minor residual strength changes from a small amount of wear are difficult to predict.

The results in this section support the applicability of our rope deterioration model for the prediction of rope life and residual strength. However, in actual tensile cycling of rope, the majority of the available rope failure data, especially for low

axial load tests, represents eye or tangential point failures(Fig. 5). Therefore, in actual prediction of rope behavior or failure life analysis, eye and tangential point failure modes should be considered.

C) Comparison of Predicted and Measured Results on External Wear Failure of Rope(Eye or Tangential Point Failure in Cyclic Loading Tests)

There is little available data on tests designed to explore the external wear effect on the rope deterioration processes. Fortunately, from the laboratory test results of Ref. 6, we can collect many eye and tangential failure data with comments of external wear evidences and testing conditions[6]. However there is no information on the contact width of rope on bollard in each test.

From the eye geometry, where the axial rope tension in the eye-spliced zone can be expressed as:

$$T_{eye} = \frac{T_{midspan}}{2\cos(\frac{D_b}{L_{end}})} \tag{3a}$$

where

$T_{midspan}$: Rope tension at mid-span

T_{eye} : Rope tension at eye-splice zone

D_b : Diameter of bollard

L_{end} : Eye zone length

Since the typical magnitude $D_b/2L_{end}$ is 0.17 - 0.25[4], the cosine term becomes 0.97-0.98 Thus under the most testing conditions

$$T_{eye} \sim 0.5\, T_{midspan} \tag{3b}$$

Since the axial rope tension in the eye is half of that of the mid-span, the predicted failure time of the eye section based only upon internal wear should be much longer than that of the mid-span. Therefore, the deterioration life of the

eye-splice part of the rope has been modelled with external wear, neglecting the internal wear contribution.

If the external wear modelling is successful, the rope deterioration model can be expanded to a rope with an eye-splice by connecting the rope model and the external wear in series. Since failure at the eye and mid-span are independent, the predicted failure life of the rope can be expressed as combined S-N curves with a doubled load scale for the eye as shown in Fig. 11a.

It is noted that the eye and tangential failure life is dependent on the bollard geometry and can be any one of curves 1,2, and 3 of Fig. 11a. When these curves are normalized with the overall rope single cycle strength, the resultant curves become curves 1, 2, and 3 of Fig. 11b. These curves can be used to explain the eye and tangent point failure data qualitatively. (Note that typical literature data are based on the overall rope initial mid-span strength even if fatigue failure is in the eye.)

An extensive external wear effect on the rope strength was reported on the bollard effect test by Bitting[16]. His result shows that the rope strength decreases when the diameter of bollard becomes bigger than 10 to 15 of of rope diameter. The rope length per primary helix cycle of a 7/8 inch rope is 10 to 12 times that of the rope radius and the rope length wound on such bollards is 31 to 45 times the rope diameter. Thus the rope length per primary helix cycle becomes 27 to 32 % of rope segment length wound on bollard. Since the nylon rope breaking strain is about 20 to 30 %, the external wear changes from local wear to uniform external wear mode as the bollard size increase. Thus, the strength reduction in a cyclic tensile test with a large bollard can be explained as in uniform external wear mode.

Predictions were made with both the simple bundle model and the uniform external wear models. The simple bundle model assumes wear on only one side on a cross-section of the rope, where the contact occurs, while the uniform external wear model assumes that wear which occurs at the contact zone reduces the effec-

tive rope diameter by the amount of wear depth, but it distributed all around the circumference. Thus, the uniform wear case assumes that strands worn away at the contact zone do not reload as they move along and around the rope. Curves B and E of the Fig. 12a and b are the simple bundle and uniform external wear model predictions are calculated for the same conditions used by Crawford[6], with an assumed contact width of 1.5 times of sheath radius which is almost 0.75 times the rope diameter. Fig 12a and b compare the predicted S-N curves to the measured external wear failure results of Crawford[4], which are the large black circles, and other collected end failure data from several different sources obtained under slightly different testing conditions[1].

As expected, the simple bundle model(B) gives longer wear life than the uniform external wear model(E) and the internal wear model for mid-span failure. The uniform external wear model reflects a similar trend to that of the data points, but is shifted to the right by a decade. There are two possible reasons for this. One is that the assumed in-contact width is too great, and the other is that there is a difference in wear S-N curves. If the failure comes from external wear at the eye and the wear S-N curves of filaments against the bollard material are similar to the yarn on yarn wear S-N data, then the S-N characteristics should show similar intercept points of log number of cycles(which represent combined value of C_o of yarn wear data and rope size). Though it is a rough estimation, the extrapolated zero load intercept points in terms of log failure cycle is about 5 for wet nylon and 6.5 for PET ropes for both the experimenal data and predictions. Thus, causes of the difference from experimental data may be due to the contact width or contact pressure assumed in computations, not to the wear resistance against the actual bollard.

These results suggest that the external wear model can explain much eye failure data in laboratory cyclic fatigue tests and give suggestions as to bollard or

rope eye design. However, the effect of the external wear must be very small for buoy mooring lines which do not contact any hard object or surface during their deployment.

D) The Effect of Low and High Load Wear Regimes

This section briefly explores the effects of yarn wear data in the low axial load range of greatest interest in most rope deployments. Fig. 13a,b.c and d are predicted S-N curves of nylon 66 and PET ropes as a function of yarn wear S-N properties, where the parameters in Fig. 4 have been varied systematically (they do not represent measured yarn data). All parameters used are listed on the plots and can be referred to Fig. 4. Fig. 13a and b are rope S-N curves as a function of P1 values, which represent low normal load wear behavior of the yarns. Fig. 13c and d show the rope S-N curves as a function of wear behavior of yarns at high normal loads. These results indicate that for simple rope tensile fatigue tests(mid-span failures), yarn wear characteristics at low normal loads dominate the rope S-N curve at low applied axial loads. However, at high axial loads, rope failure depends mostly on the tensile creep behavior of the component fiber, and, therefore, filament wear behavior shows no effect on the rope S-N curve. If the parameters used in the calculations give reasonable values of normal pressure, this result is especially important in actual ropes because according to industry specifications most ropes are deployed in the low load regime. It is concluded that study is needed of the basic yarn wear behavior at low loads, and any yarn improvements in this area would greatly improve rope performance.

5. CONCLUSIONS

In this study, prediction of deterioration life of synthetic double braided rope has been conducted with an ideal geometrical model[12] considering two major rope deterioration factors: tensile creep fatigue and wear behavior of constituent fibers.

Comparisons have been made between predicted values with available measured values. From such comparisons the following can be concluded:

1) The predicted S-N curves of ropes deterioration life shows two regimes; one is dominated by fiber wear failure at the low load regime and the other by tensile fatigue of fibers, at the high load regime. The relative extent of these two portions in a S-N curve depends on wear characteristics, structure, and relative frequency of tensile cycling.
2) The tensile strength of a rope can be affected by internal wear during a single monotonic tensile loading. This is predicted in rope deterioration model. The ultimate breaking load as affected by internal wear is actually measurable breaking strength.
3) Predicted rope S-N curves and residual strengths of strands and ropes demonstrate reasonably close values to the actually measured experimental data.
4) An improvement of yarn wear property at low normal load will increase the predicted rope life for low rope tensile loads. However, improvement of yarn wear life at high normal load does not increase predicted rope life at high rope tensile loads. Since the typical safety factors of ropes are 5 to 10 in marine environments, it suggests that the improvement of low load wear life is crucial in actual mooring deployment life.
5) A qualitative rope failure models including uniform external wear at the eye, can explain eye and tangential point failure during rope cyclic tensile fatigue tests due to external abrasion.

References

[1] Bitting, K., "Physical Properties of 3-7 year old Nylon Double Braided Buoy Moorings", U.S.C.G. report Oct. 1983

[2] Bitting, K.,"Full-Scale Test of A Synthetic Line Mooring", Interim Report,

project 732484.02, Nov. 1983

[3] Parsey, M., "Fatigue Resitance and Hysteresis of Manmade Fiber Rope", Society of Petroleum Engineers, Offshore Europe Conference, Aberdeen(1983)

[4] Flory, J.,"OCIMF Hawser Test Standards Development Program, Trial Prototype Rope Test", Final Report, Oil Companies International Marine Forum, October(1983)

[5] Werth, J. L., "An Evaluation of Material and Rope Construction for Mooring Hawser Design", Proc. Offshore Technology Conference, Houston, paper 3851, 497-507, 1980

[6] Crawford, H. and McTernan, L. M., "Cyclic Testing of Continously Wetted Synthetic Fiber Ropes", Offshore Technology Conference, Houston. Paper 4635, 455-466, 1983

[7] Gibson, P. T. and Wolfe, H. D., "Cyclic Tension Fatigue Performance of Synthetic Fiber Ropes", Final Report of Contact N62306-82- M2195, 10th Jan. 1984

[8] Samson Ocean Sytem, "Cyclic Testing of a 6" Circumference Stable Braid (wet condition).", TR-64-84, 23th, Oct., 1984

[9] Backer, S. and Seo M. H., "Mechanics of Degradation in Marine Rope", Proceedings of the Third Japan-Australia Joint Symposium on Objective Measurement: Applications to Product Design and Process Control, Kyoto, Japan, September 5-7, 1985, 63

[10] Kenney, M. C.,Mandell, J. F.,McGarry, F. J.,"Fatigue Behavior of Synthetic Fibers,Yarns, and Ropes", J. Mater. Sci., 20, (1985)2045-2059

[11] Steckel, M. G., "Tensile Fatigue Behavior of Polyester Yarns in Ambient and Sea Water Environments", MS thesis, M.I.T. 1982

[12] Seo, M. H., "Mechanical Deterioration of Synthetic Fiber Rope in Marine Environment", Ph.D. Thesis, The Department of Mechanical Engineering,

Massachusetts Institute of Technology (1988)

[13] Backer, S. and Hsu, P., "Structures with Partial Frictional Constraints", Proceedings of the Third Japan-Australia Joint Symposium on Objective Measurement: Applications to Product Design and Process Control, Kyoto, Japan, September 5-7, 1985, 63

[14] Hearle, J. W. S. and Grosberg, P.,Backer, S., Structural Mechanics of Fibers, Yarns and Fabrics. Wiley-Interscience , New York 1969

[15] Mandell, J. F., "Modelling of Marine Rope Fatigue Behavior" Text. Res. J., vol. 47, 318-330, 1987

[16] Bitting, K. R., "The Bollard Efficiency of Nylon and Polyester Lines", U.S. Coast Guard Report, Groton, CT, October, 1983

[17] Chen, J., "Three-Strand Rope Behavior in Tension and Torque", S.M. Thesis, The Department of Mechanical Engineering, Massachusetts Institute of Technology (1988)

[18] Hsu, P., "Fracture Mechanisms of Synthetic Fiber Ropes", Ph.D. Thesis, The Department of Mechanical Engineering, Massachusetts Institute of Technology (1984)

[19] Toney, M., "On the Mechanical Behavior of Twisted Synthetic Ropes", S.M. Thesis, The Department of Mechanical Engineering, Massachusetts Institute of Technology (1986)

[20] Wu, H. C., "Modelling of Fibrous Assemblies- Tensile and Bending Behavior", Ph.D. Thesis, The Department of Materials Science and Engineering, Massachusetts Institute of Technology (1990)

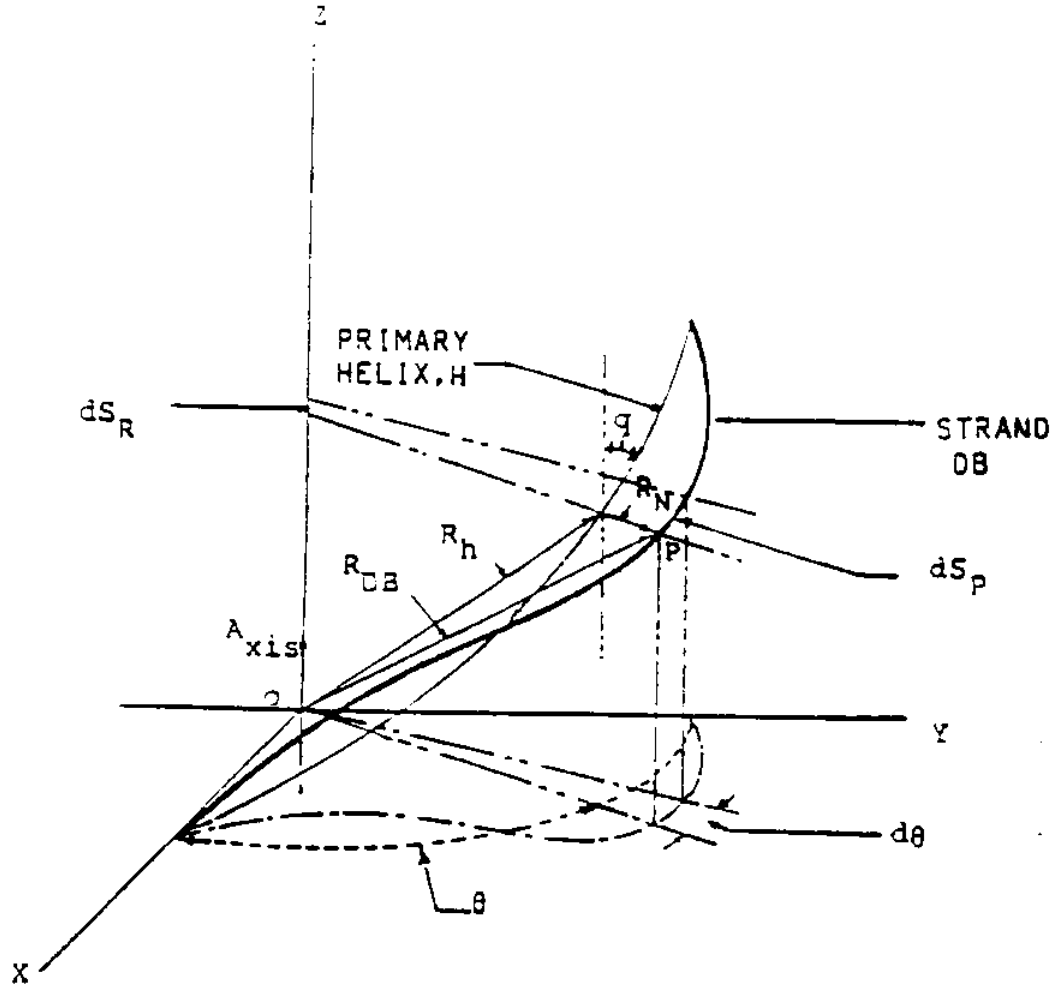

R_{DB} : POSITION VECTOR OF A POINT P ON A STRAND

R_h : POSITION VECTOR OF PRIMARY HELIX

R_N : SINUSOIDAL UNDULATION VECTOR

A_{xis} : ROPE AXIS VECTOR

q : HELIX ANGLE

θ : BASE ANGLE

dS_p ,dS_R : DIFFERENTIAL LENGTHS OF STRAND AND ROPE AXIS

Figure 1 : Diagram of Model Strand Path

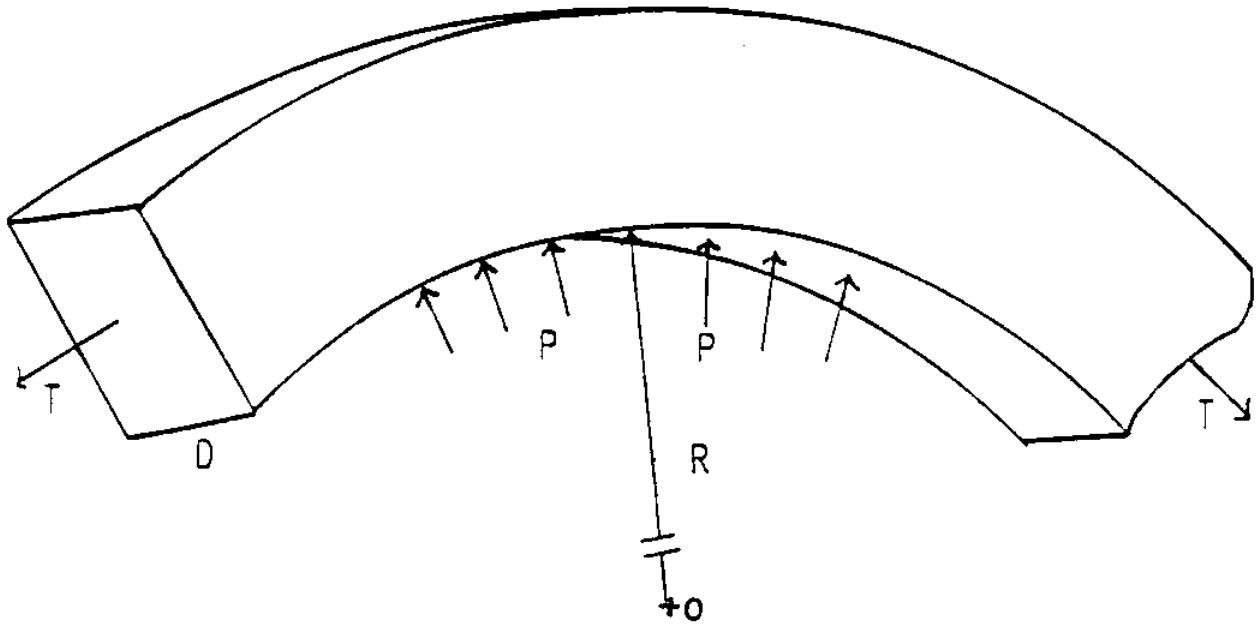

N : NUMBER OF FILAMENTS ON CONTACT AREA

T : TENSION

K : CURVATURE

R : RADIUS OF CURVATURE

D : CONTACT WIDTH

D_F : DIAMETER OF FILAMENT

P : PRESSURE OF CONTACT AREA

$$P = T \times K / D$$

$$D = N \times D_F$$

Figure 2 : Diagram of Square Bundle Model of Deterioration

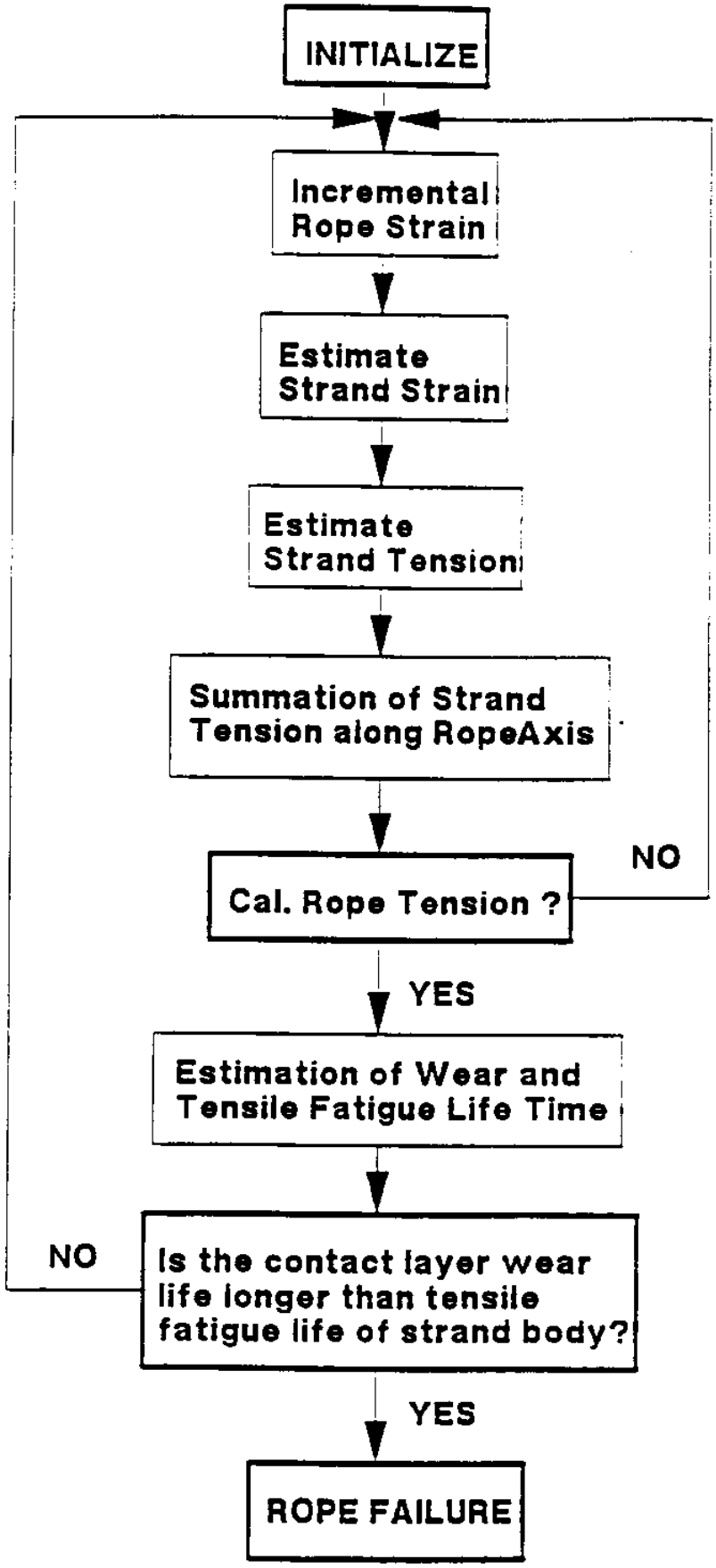

Figure 3 : Program Flow Diagram

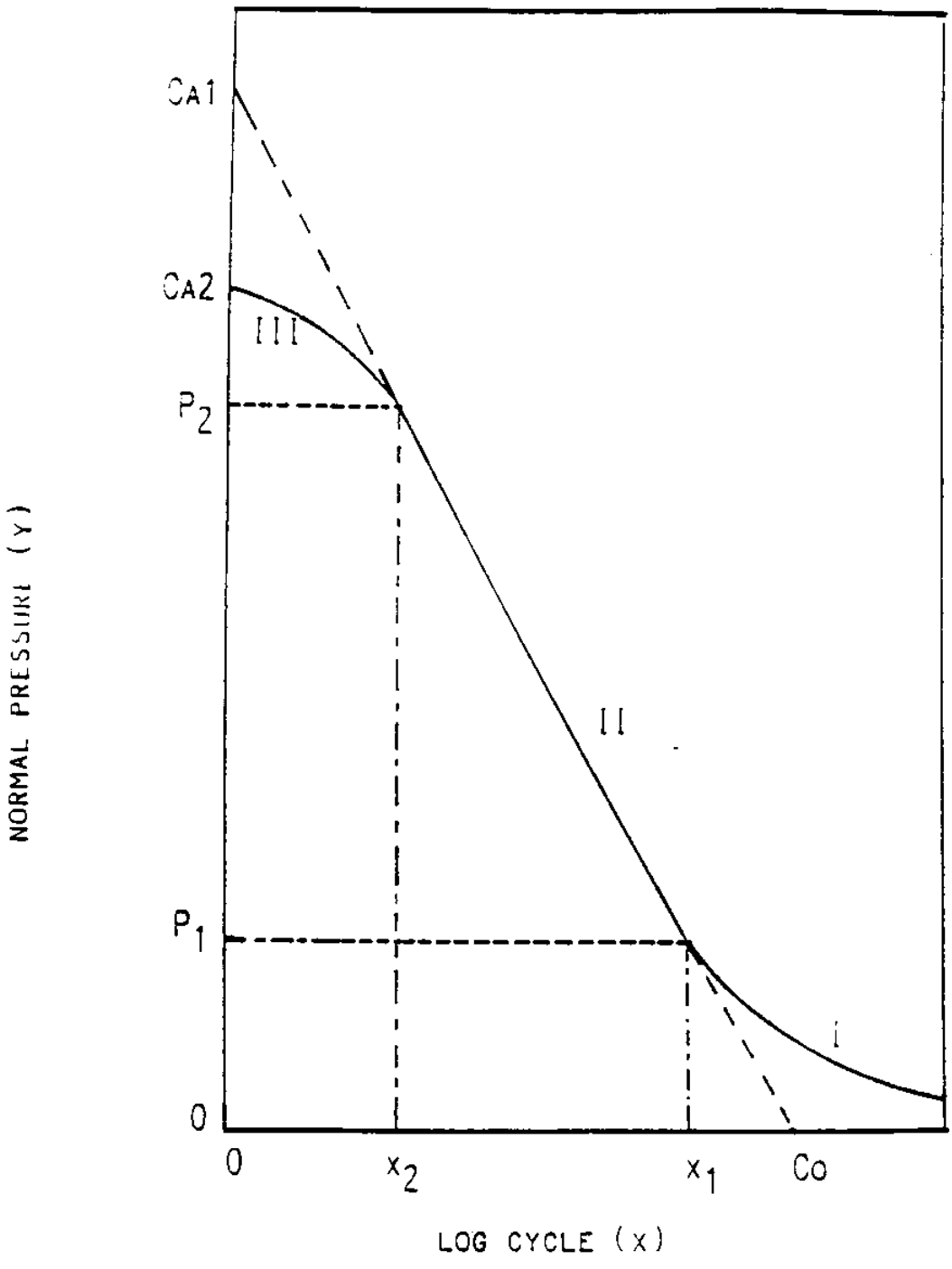

Figure 4 : Three Segment Model of Filament Wear S-N Curve

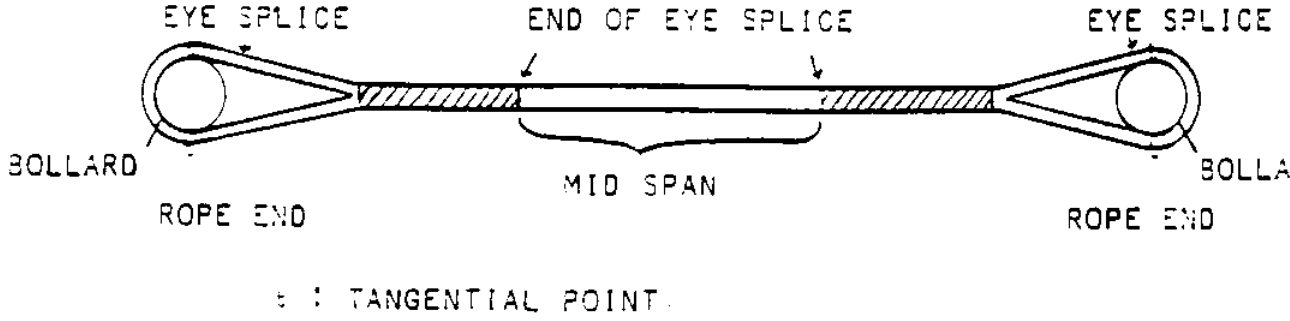

Figure 5 : Diagram of Rope Specimen

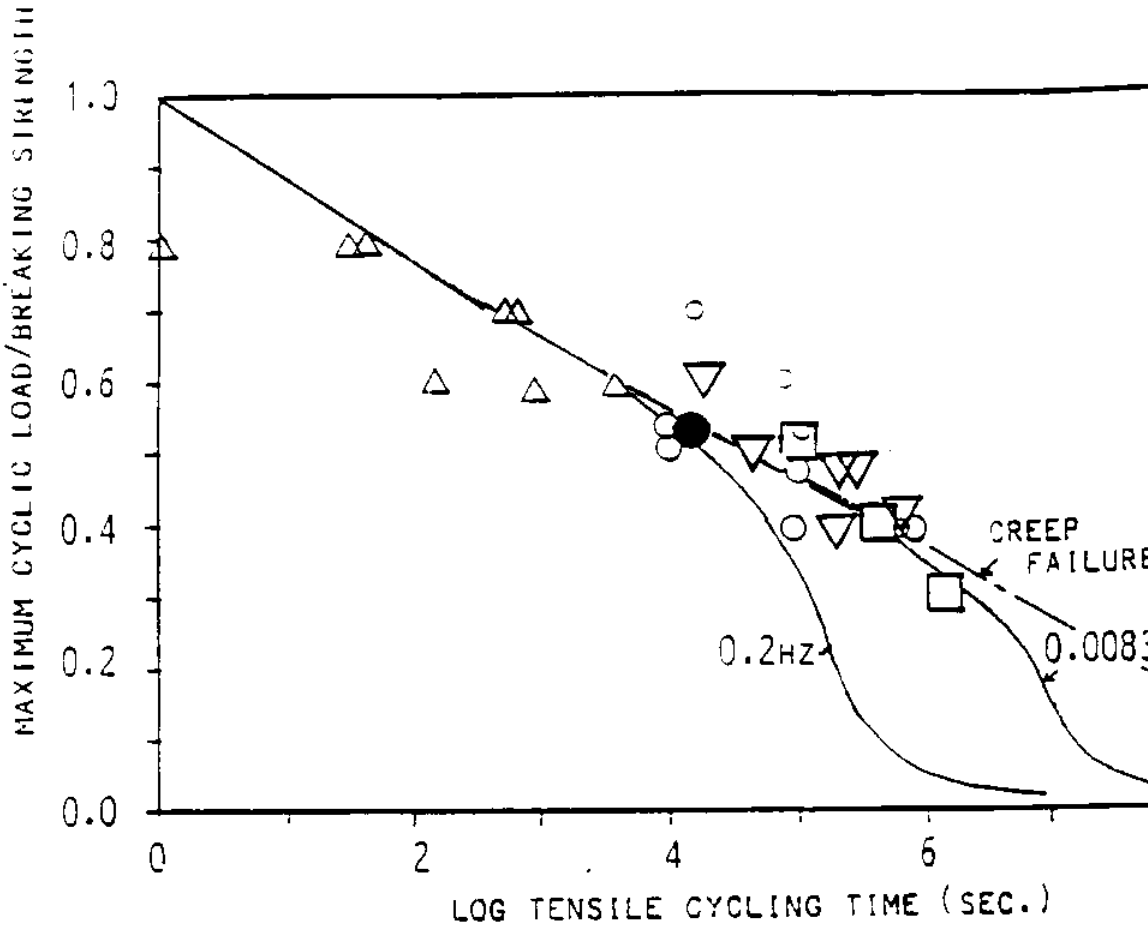

	CONST.	DIA.(MM)	CYCLE PERIOD(SEC
●	DBR	18	2
△	DBR	4.8	2
▽	DBR	120	120
○	DBR	48	45
○	DBR	24	80
□	DBR	64	90

Figure 6 : Comparison of Predicted Wet Nylon Rope S-N Curve with Measured Results [6]

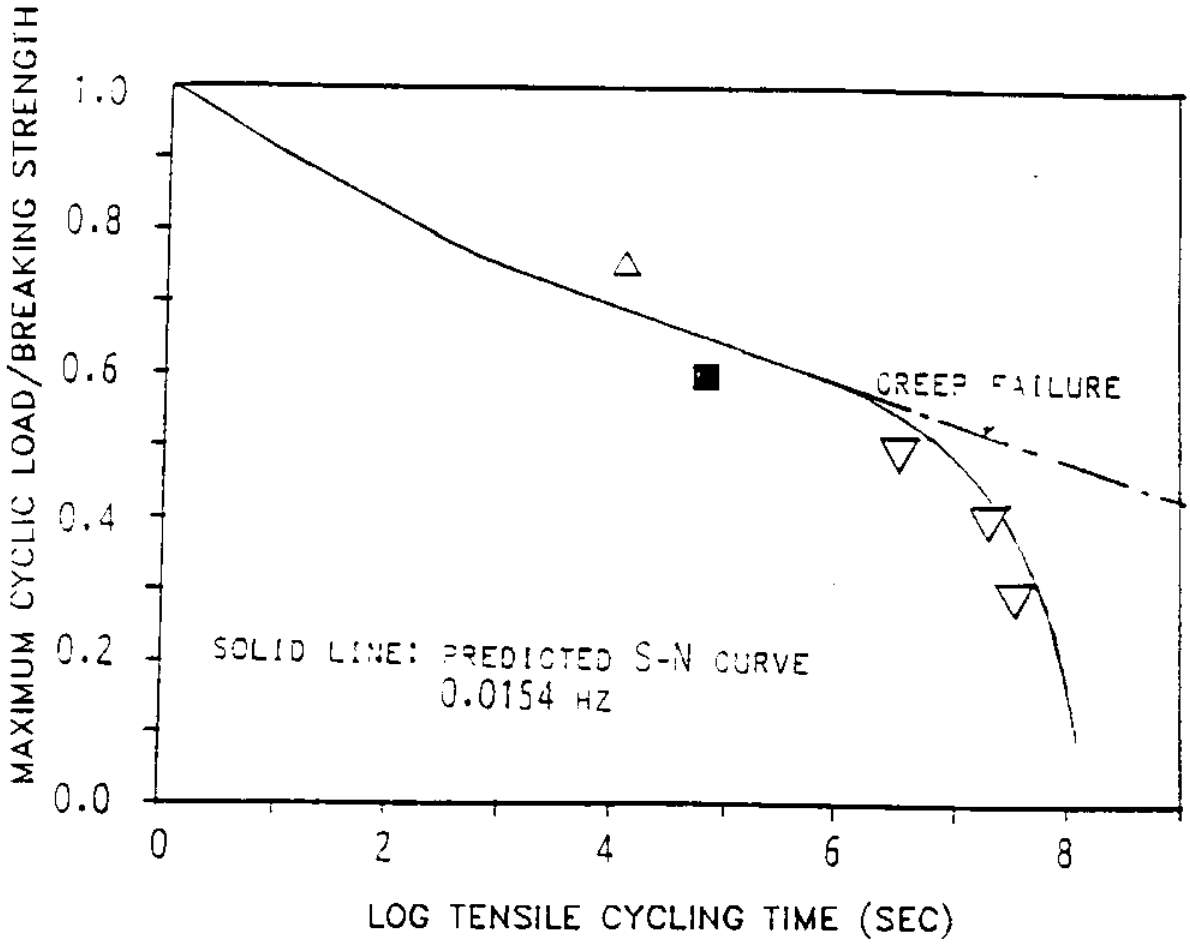

	CONST.	DIA.(mm)	CYCLE PERIOD(sec)
△	DBR	18	2
▽	DBR	24	65
■	DBR	50	10

Figure 7 : Comparison of Predicted Wet PET Rope S-N Curve with Measured Results [6]

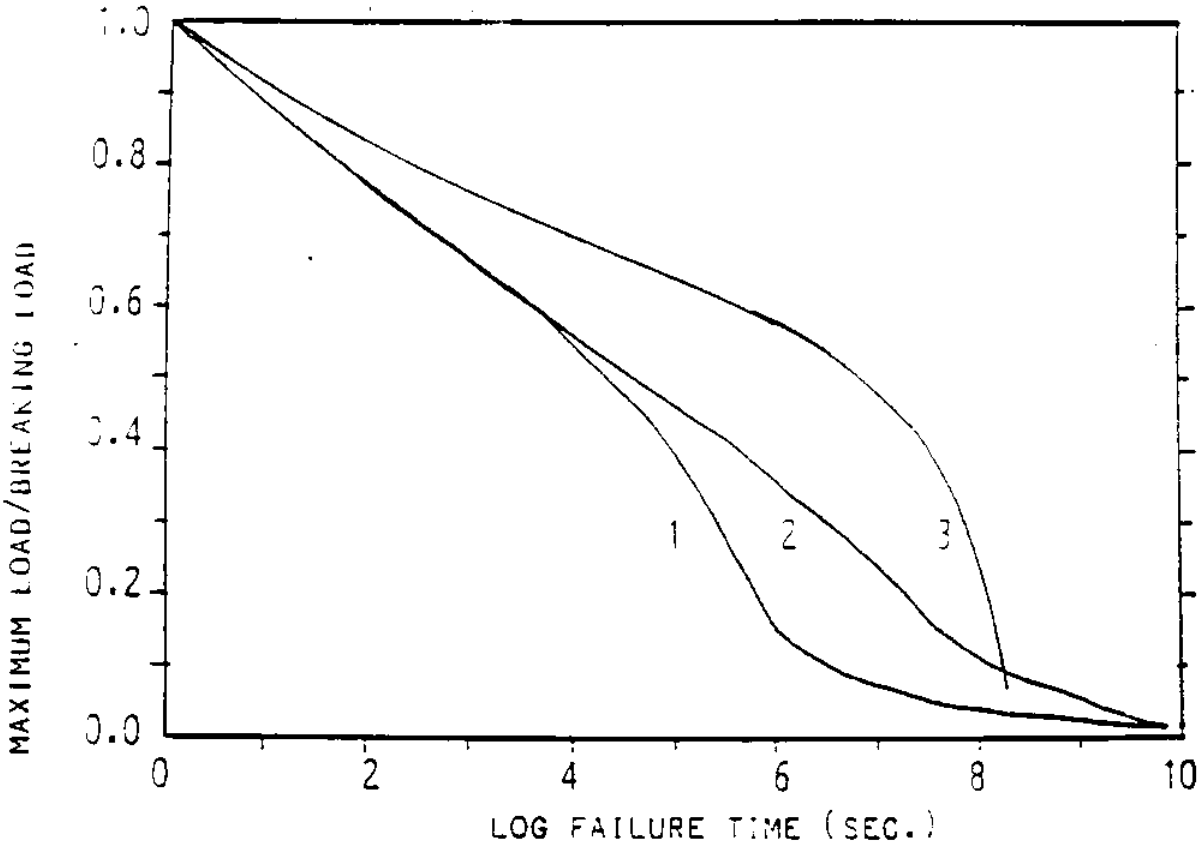

* 1: NYLON WET 0.2 HZ
2: NYLON WET 0.00833 HZ
3: PET WET 0.0154 HZ

Figure 8 : Comparison of Predicted S-N Curves of Wet PET and Wet Nylon

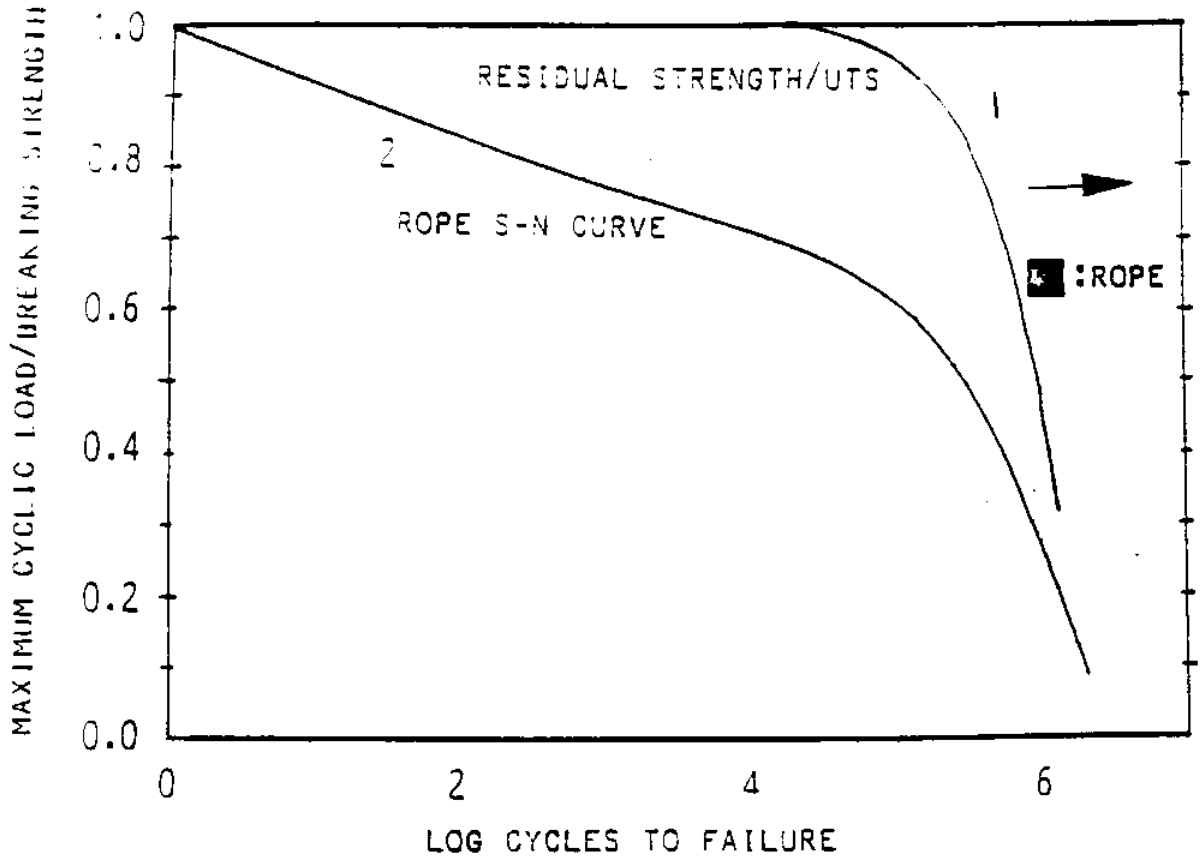

Figure 9 : Predicted Residual Strength and Rope S-N Curves of Samson PET Rope Wet Tested Cyclically to 25% of UTS at .0935 Hertz [8]

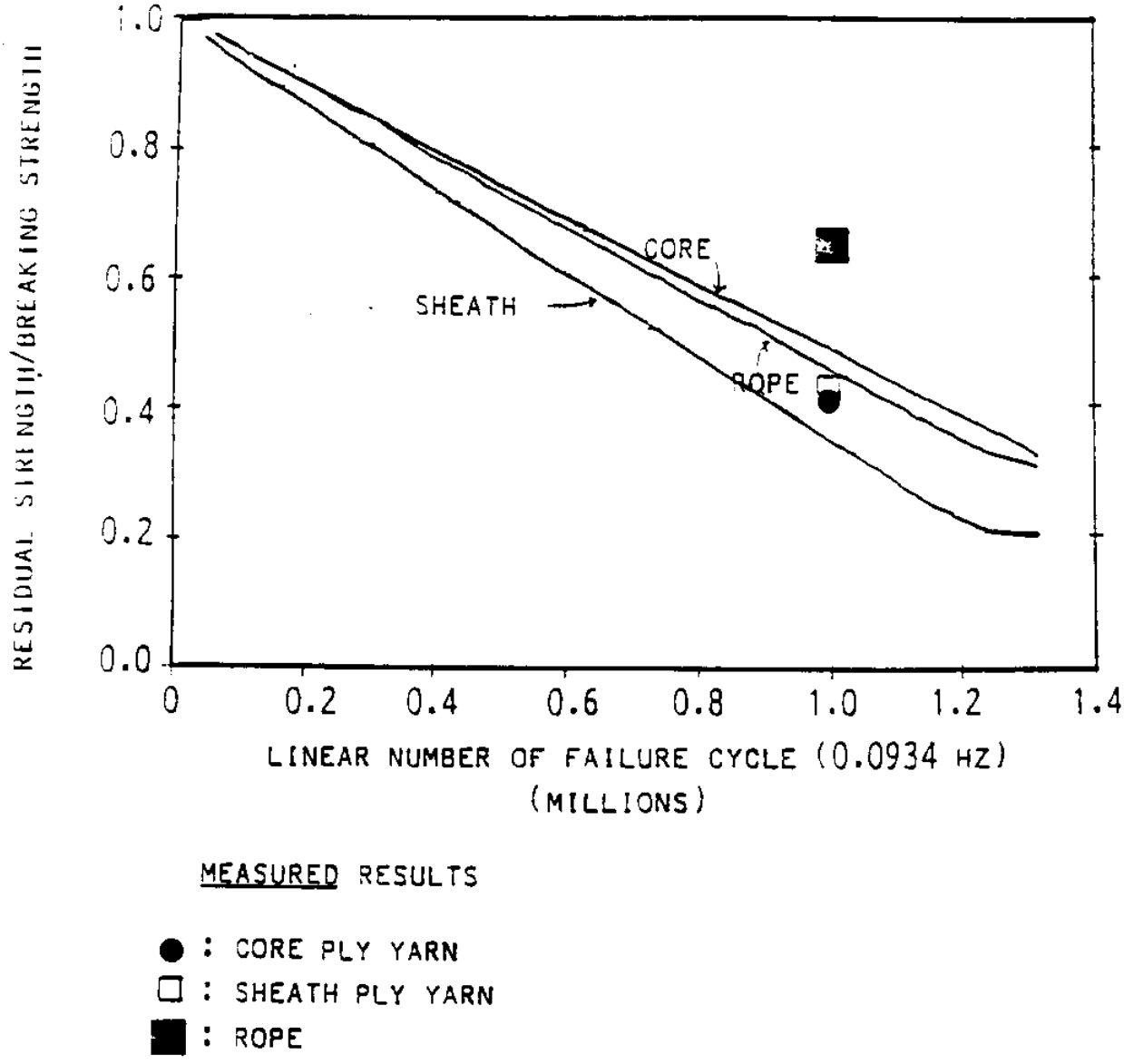

Figure 10 : Predicted and Measured Residual Strength of Samson PET Rope as a Function of Number of Cycles

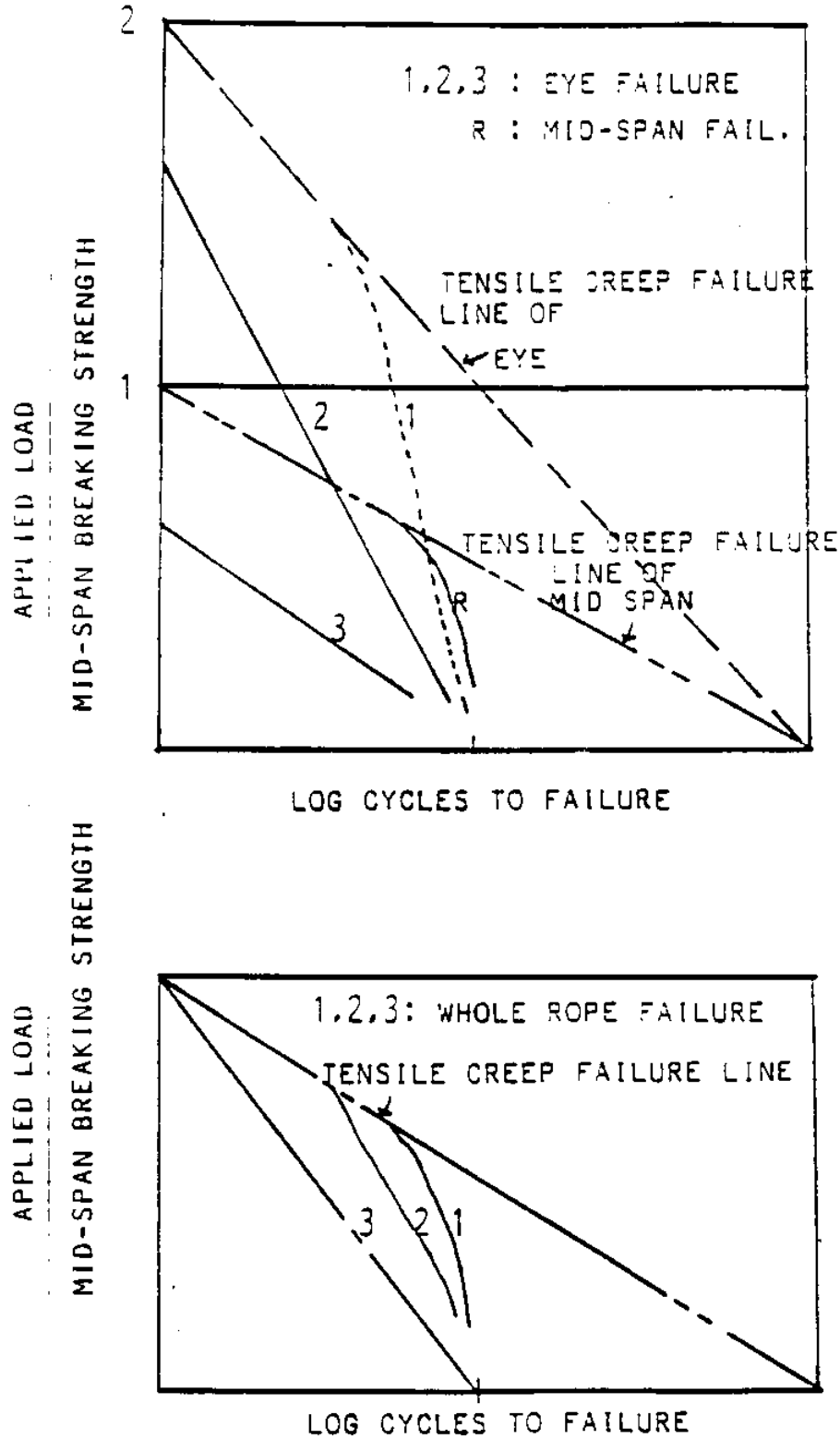

Figure 11a,b : Failure in Rope and Eye Splice Series Model

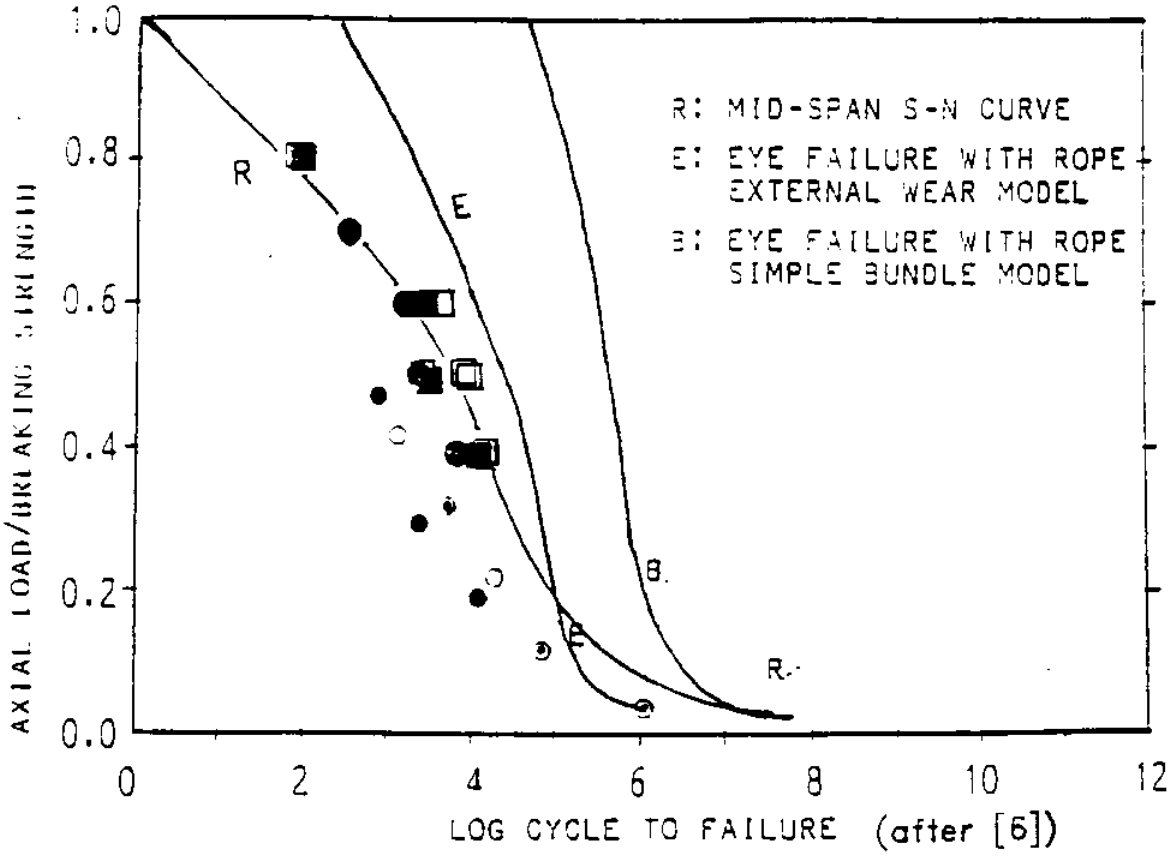

* contact width at eye splice : 1.5 x sheath radius
* D/2L = 0.25

Figure 12a : Comparison of Predicted vs. Experimental Values for Rope Eye Splice Failure Cycles (Nylon: 80 sec/cycle)

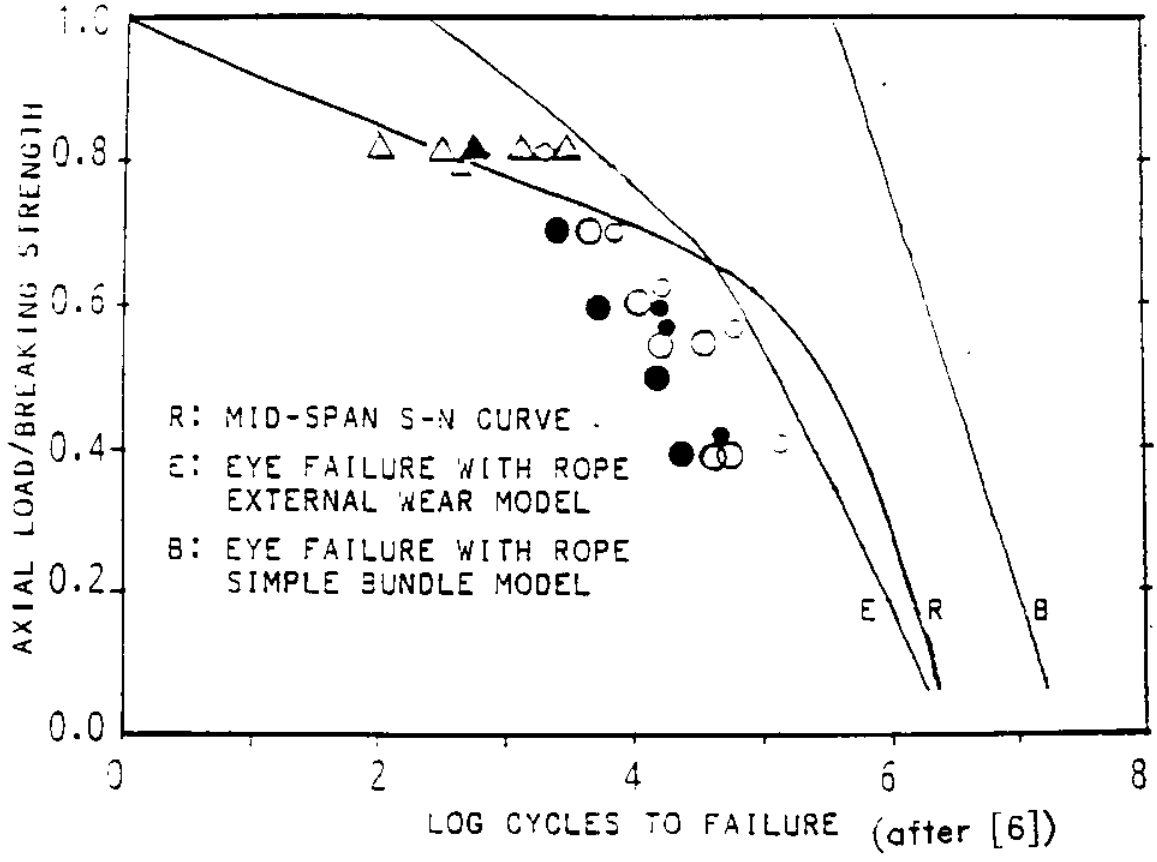

* contact width at eye splice : 1.5 x sheath radius
* D/2L = 0.25

Figure 12b : Comparison of Predicted vs. Experimental Values for Rope Eye Splice Failure Cycles (PET : 65 sec/cycle)

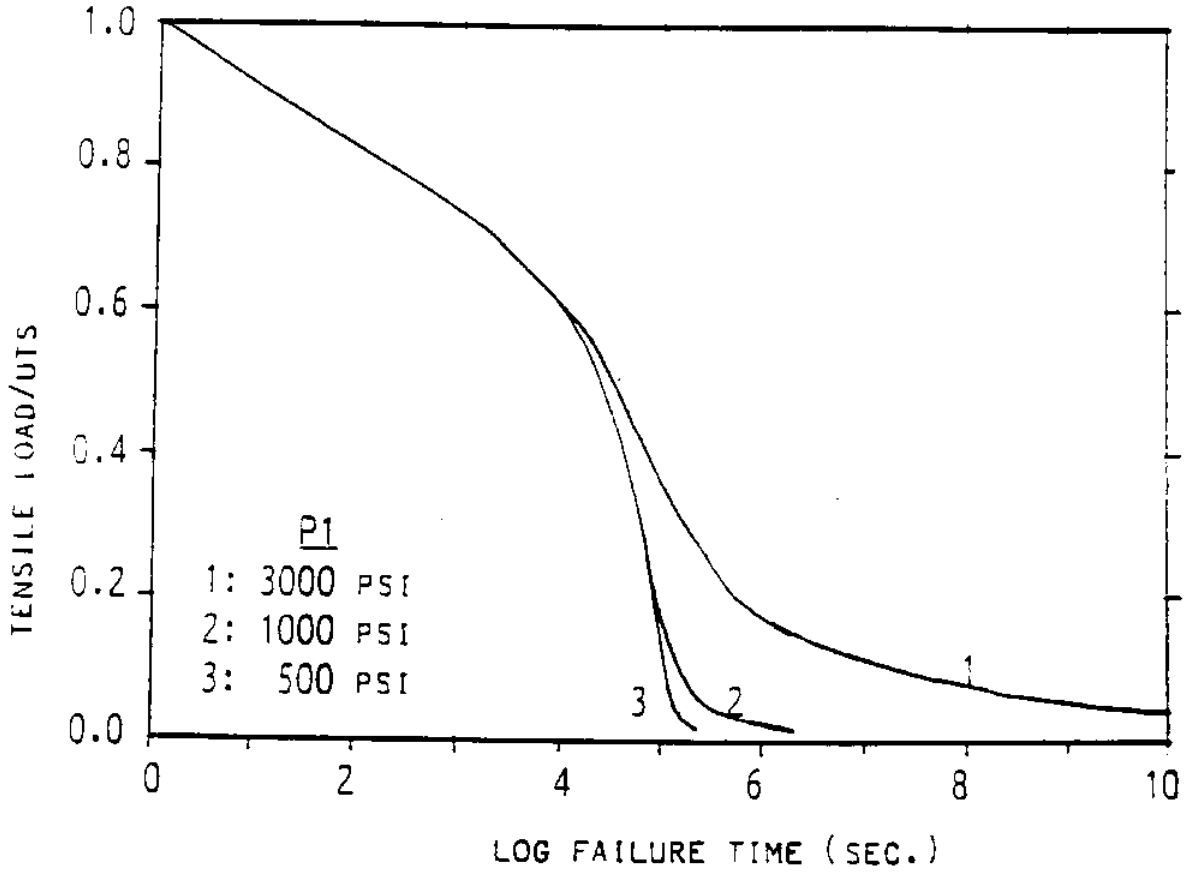

Parametric Conditions

$P2 = 6750$ psi $C_O = 3.6$ log cycles

$C_{A1} = 21350$ psi $C_{A2} = 18000$ psi

$S_T = 10$: Tensile Fatigue S–N Slope

Figure 13a : Predicted Effect of Wear Resistance of Filaments at Low Normal Loads on the 7/8" dia. Double Braided Rope (Wet, 707 Nylon)

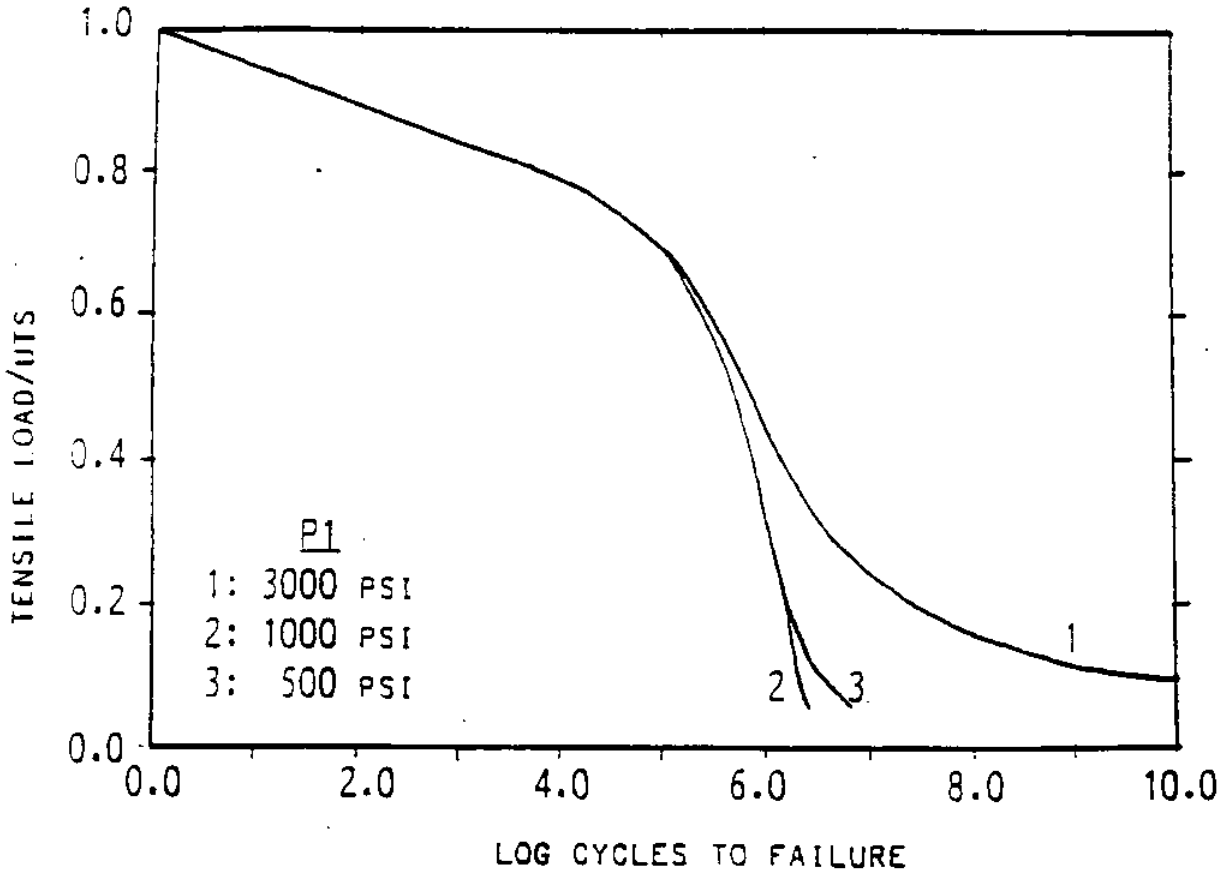

Parametric Conditions

P2 = 9900 psi C_O = 4.5 log cycles

C_{A1} = 18150 psi C_{A2} = 16850 psi

S_T = 17.54 : Tensile Fatigue S–N Slope

Figure 13b : Predicted Effect of Wear Resistance of Filaments at Low Normal Loads on the 7/8" dia. Double Braided Rope (Wet, 608 PET)

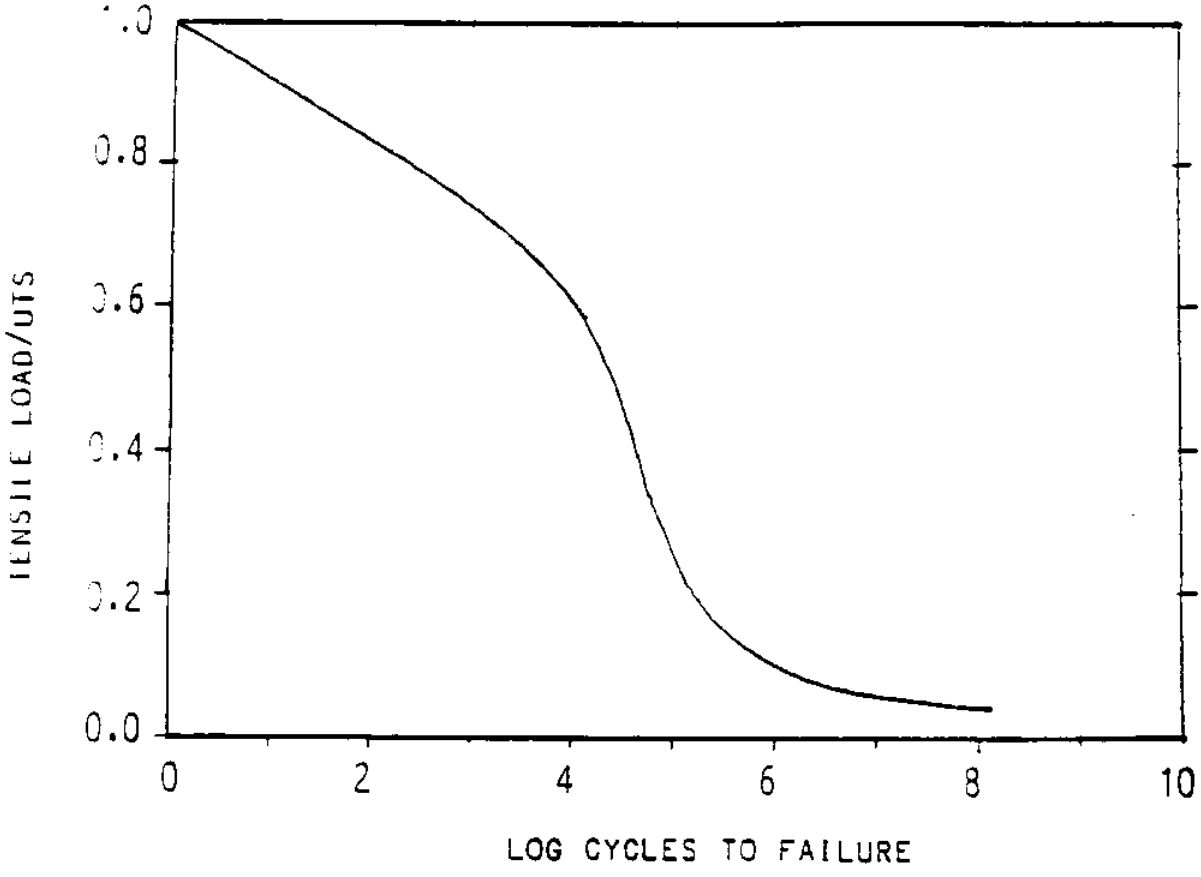

Parametric Conditions

P1 = 2250 psi P2 = 5000 ~ 22000 psi

C_{A1} = 21350 psi C_{A2} = 8000 ~ 23000 psi

C_0 = 3.6 log cycles (no effect of variations)

S_T = 10 : Tensile Fatigue S–N Slope

Figure 13c : Predicted Effect of Wear Resistance of Filaments at High Normal Loads on the 7/8" dia. Double Braided Rope (Wet, 707 Nylon)

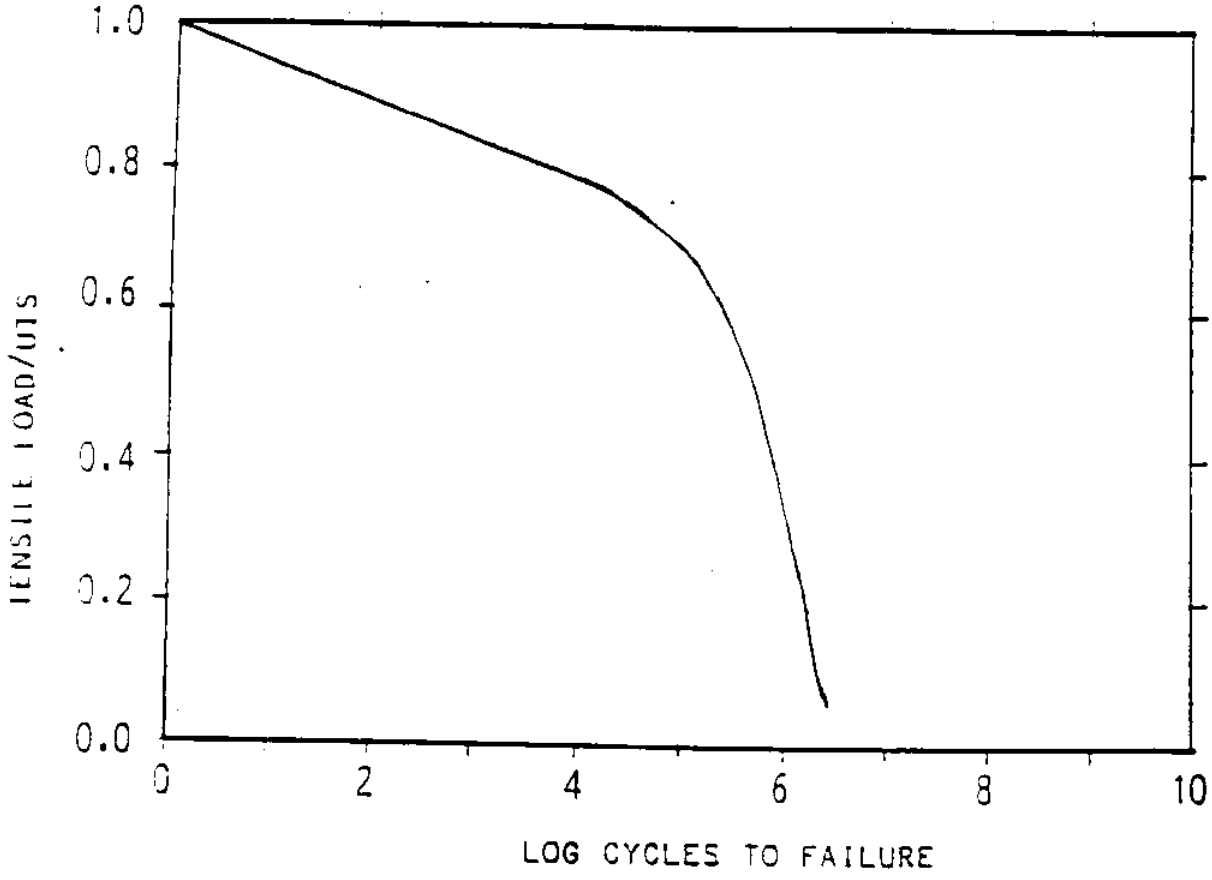

Parametric Conditions

P1 = 500 psi P2 = 5000~15000 psi

C_{A1} = 18150 psi C_{A2} = 8000~18000 psi

C_0 = 4.5 log cycles (no effect of variations)

S_T = 17.54 : Tensile Fatigue S-N Slope

Figure 13d : Predicted Effect of Wear Resistance of Filaments at High Normal Loads on the 7/8" dia. Double Braided Rope (Wet, 608 PET)